Are hubs differentially affected in early versus late onset AD? A study based upon the minimum spanning tree of functional EEG networks

H de Waal, WM van der Flier, P Scheltens, CJ Stam, ECW van Straaten

Submitted

Chapter 5

Abstract

Introduction
Aim of this study was to investigate with a novel method of brain network characterization, the minimum spanning tree (MST), whether functional hub regions are lost in AD. Furthermore, we investigated whether age-at-onset of disease modified the loss of hubs.

Method
We examined resting state EEGs of 319 probable AD patients and 245 non-demented controls, categorized into young (≤65 years, age: AD 59(5); controls 55(7)) and old (>65 years, age: AD 75(5); controls 72(4)). Phase Lag Index (PLI) in four different frequency bands (alpha, beta, theta and delta) was used as connectivity measure, from which we calculated the MST as a simple, non-arbitrary way to represent functional brain networks. Cognition was measured with digit span forward and backward, Visual Association Test (VAT) naming and recall, Trailmaking Test (TMT) parts A and B and category fluency. We used Analyses of Variance (ANOVA) for group comparisons. We used ANOVA for repeated measures to study potential difference in distribution of hubs (BC per electrode) according to age-at-onset in AD patients and controls separately. Correlations with cognition in AD patients were established by Pearson's correlation coefficient.

Results
AD patients showed in the alpha band a lower degree and leaf fraction and higher eccentricity and diameter compared to controls. We found no differences in BC per electrode according to age in controls, but younger AD patients had stronger hubs left temporal and weaker hubs left occipital than older AD patients. We found alpha band correlations between diameter and category fluency, VAT recall and digit span backward (resp. r = 0.12, -0.12 and 0.13), between eccentricity and category fluency, VAT recall and digit span backward (resp. r = 0.13, 0.12 and 0.13) and between leaf fraction and category fluency, VAT recall and TMT B (resp. r = -0.13, 0.12 and -0.14) in the group of AD patients.

Conclusion

In this study we have shown with MST, a novel method of network analysis in EEG, that AD patients have a different, less integrated network topology compared to controls, which is consistent with loss of hubs, higher connected areas that have been implicated in the pathophysiology of AD, and seems related to severity of cognitive impairment. Further more, in AD patients there was a difference according to age in hub locations; young AD patients had stronger hubs left temporal than old patients and weaker hubs left occipital.

Introduction

An optimal segregation and integration of information flow in the brain is necessary for optimal cognitive functioning.[1] Disruptions of this balance are associated with several disorders including Alzheimer's disease (AD), which has been referred to as a disconnection syndrome.[2,3] In recent years many studies were published that describe brain dynamics in terms of complex networks using imaging methods like functional MRI (fMRI) and magnetoencephalography (MEG).[4-6] Highly connected hub-regions are increasingly recognized as playing an important role in the efficient integration of information.[7-9] Studies in several imaging modalities have shown an increased vulnerability of hub-regions to AD related pathology and loss of optimal network configuration in AD patients.[10-18] Changes in network properties have also been shown to correlate with cognitive decline in Alzheimer's disease.[19-21]

AD is the most common cause of dementia.[22,23] Within AD there is a marked heterogeneity in clinical presentation. While most patients with late onset AD present with memory problems, an early age at onset of AD is more often associated with problems in other cognitive domains.[24-26] In addition to a different clinical phenotype, it has also been shown that young AD patients show regional differences in cerebral atrophy, glucose metabolism and amyloid deposition, with the posterior brain regions most affected.[27-29] In a recent electroencephalography (EEG) study, we showed that young AD patients had more slowing of oscillatory brain dynamics in the posterior brain regions, compared to old AD patients.[30] Taken together, these findings suggest that connections in the brain of older and younger patients are differently affected. The predilection for a posterior localisation of pathology in young AD patients possibly represents damage to the posterior part of the Default Mode Network (DMN). Since it is known that many hub regions are located in the DMN,[10] it could be hypothesized that in young AD patients, a disproportionate number of hub regions is affected compared to old AD patients. The mechanism through which this occurs is not yet known, but differences in functional network topology could be an underlying factor, as it has been shown that hub vulnerability is likely caused by the high activity level of these regions, also known as activity dependent degeneration (ADD).[31]

In this EEG-based study we used a novel unbiased method of network characterization that gives a hypothesis-free characterization of the network, the Minimum Spanning Tree (MST), to investigate whether AD is associated with loss of hubs and whether this association is modified by age-at-onset. In addition, we studied whether network measures were related to cognitive impairment.

Methods

Subjects

We included of 319 probable AD patients (F 49%; MMSE 21(5)) and 245 non-demented controls (F 45%; MMSE 28(2)) from the memory-clinic based Amsterdam Dementia Cohort, similar to the dataset used in previous studies.30,32 All subjects were referred to the Alzheimer center of the VU University Medical Center, Amsterdam, the Netherlands, between September 2003 and June 2009.

Standardised dementia screening included a history, and when available, an informant based history, a standard neurological examination, a cognitive examination including mini mental state examination (MMSE), neuropsychological examination (including digit span forward and backward, Visual Association Test (VAT) naming and recall, Trailmaking Test (TMT) parts A and B and category fluency),[33-36] EEG, Magnetic Resonance Imaging (MRI) of the brain and screening laboratory tests. Patients were diagnosed with probable AD during a multidisciplinary consensus meeting, according to the NINCDS-ADRDA criteria.[37] All patients also met National Institute on Aging-Alzheimer's Association (NIA-AA) core clinical criteria.[38] The control group consisted of patients who presented at our memory clinic with subjective complaints, but who had normal clinical investigations and did not have significant cognitive deficits (i.e. Mild Cognitive Impairment criteria were not fulfilled)[39] or major psychiatric disorder. Both AD patients and controls were categorized according to age in a young group (65 years or younger at time of diagnosis) and an old group (older than 65 years at time of diagnosis). All patients gave written informed consent for the storage of the results of the examinations in a local database and for the use of the data for research purposes. This protocol was in agreement with the

WMA declaration of Helsinki, and approved by the ethical review board of the VU University Medical Centre.

EEG recording

All EEGs were recorded using the OSG digital equipment (Brainlab®; OSG b.v., Rumst, Belgium) at the positions of the 10-20 system: Fp2, Fp1, F8 F7, F4, F3, A2, A1, T4, T3, C4, C3, T6, T5, P4, P3, O2, O1, Fz, Cz, Pz, with an average reference which included all electrodes, except Fp2, Fp1, A2 and A1. Electrodes A1 and A2 were not included in further analyses. Sample frequency was 500 Hz. Electrode impedance was below 5 kΩ. Initial filter settings were: time constant 1s; low pass filter, 70 Hz. Patients were seated in a slightly reclined chair in a sound attenuated room. They sat mainly with eyes closed, EEG technicians were alert on keeping patients awake by sound stimuli.

From each EEG, 4 epochs of 4096 samples of artefact free data (containing no eye blinks, slow eye movement, excess muscle activity, ECG artefacts, etc.) were selected by visual inspection (HdW). This is sufficient to obtain stable values of quantitative EEG measures.[40]

Functional connectivity

Functional connectivity was assessed with the Phase Lag Index (PLI). The PLI is a measure of statistical interdependencies between time series based upon the asymmetry in the distribution of instantaneous phase differences.[41] It reflects the strength of the coupling, and is less sensitive to volume conduction and the influence of active reference electrodes than most other frequently used measures for functional connectivity.[41] The PLI ranges between 0 and 1, a PLI value of zero indicates no coupling and a PLI of 1 refers to maximal phase-lagged coupling. The PLI was calculated in Brainwave software version 0.9.76 (in house developed by CS; further information and free available software: http://home.kpn.nl/stam7883/brainwave.html), in four frequency bands (delta band 0.5-4 Hz, theta band 4-8 Hz, alpha band 8-13 Hz and beta band 13-30 Hz). For each epoch the PLI between all possible electrode pairs was calculated, which can be represented by a connectivity matrix of 19 by 19.

Minimum Spanning Tree

To study the organisation of functional brain networks, connectivity matrices can be represented by graphs. A graph consists of nodes and edges, which are the connections between these nodes. In this study the nodes represent the EEG electrodes and the strength of the connectivity between each pair of electrodes, the PLI, represents the edge weights. In graph theoretical studies, it has proven to be difficult to compare networks across different groups and studies. Often a normalization step is required, commonly performed through thresholding or the observed networks are compared to randomized networks. These methods do not provide a unique or consistent solution.[42,43] Therefore, we used the MST to characterize network topology. The MST of an undirected weighted graph is **a unique sub-graph** that connects all nodes in such a way that the total cost (the sum of all edge weights) is minimized without forming cycles.[44] In our case, we searched for the tree with the maximum connection strength (highest PLI) for each connectivity matrix, equivalent to an MST as obtained by Kruskal's algorithm.[45] In short, the algorithm first orders the connection strength between each pair of nodes in an ascending way. Then, the construction of the tree is started with the edge with the highest connection strength (PLI). Consecutive highest connected edges are added until all nodes (n) are connected to the tree without forming cycles. If adding an edge would result in forming a cycle, that edge is disregarded. This results in a sub-graph of n nodes and n-1 edges, in our case 21 nodes (for the number of EEG electrodes) and 20 edges. In figure 1 different tree topologies are schematically represented.

To further characterize the MST, the following measures were calculated:[46] degree, leaf fraction, diameter, betweenness centrality (*BC*), eccentricity and hierarchy.

Degree is the number of edges of node i. We normalized the degree by dividing the degree by the total number of edges, which resulted in a degree that was independent of the size of the MST, to facilitate comparison with MSTs of different size. We used the maximum degree to represent the degree of the whole MST. Leaf number is defined as the number of nodes with a degree of exactly 1. The lower bound for the leaf number is 2, forming a path-like topology and the upper bound m = n-1, forming a star-like topology. We used the

leaf fraction to correct for the size of the tree, which is the leaf number divided by the maximum possible leaf number. The leaf number is related to the diameter, the largest distance between any two nodes, of the tree, where the upper limit of the diameter is defined as dmax = m – leaf number + 2, which implies that the value of the largest possible diameter decreases when the leaf number increases, and the lower bound as: 2 * (n-1) / leaf number. The BC of a node i is the number of shortest paths between any pair of nodes h and j that are running through i, divided by the total number of paths between any pair of nodes j and h. BC ranges between 0 and 1. Eccentricity of a node is defined as the longest distance between that node and any other node of the tree and is low if this node is central in the tree. Both BC and eccentricity are measures of centrality. To be able to compare centrality measures between subject groups, the maximum BC of the MST was used together with the average MST eccentricity. Figure 1 depicts several different tree topologies. The tree at the left forms a line-like topology where every node has a maximum degree of 2. The right tree represents a star-like topology with shortest possible average path length of 2. For optimal performance of a network, it has to satisfy two criteria. First, information from any node to any other node needs to be transferred as efficiently as possible, so preferably through the fewest possible links (a star-like topology). However, the central nodes in a star-like topology are vulnerable to overload, therefore the second criterion would be prevention from overloading hubs by setting a maximal BC (BCmax) for any of the nodes. The optimal tree should then reflect the best possible balance between both criteria, which could be reflected by the middle tree in figure 1. To this aim, tree hierarchy was developed to show the balance between diameter reduction and overload prevention:[46]

$$hierarchy = \frac{\text{leaf number}}{2mBC_{max}}$$

To assure hierarchy ranges between 0 and 1, the denominator is multiplied by 2. If leaf number = 2, that is, a path-like topology, and m approaches infinity, hierarchy approaches 0. If leaf number = m, that is, a star-like topology, hierarchy is equal to 0.5. For leaf numbers between these two extremes, hierarchy can have higher values with a maximum of 1.

Weighted graph analysis

Two often used measures are the clustering coefficient C and average shortest path length L.[47] The clustering coefficient is defined as the likelihood that the neighbours of a certain node are also neighbours of each other. The weighted equivalent of the clustering coefficient is the C_w.11 The path length denotes the average number of edges of the shortest path between pairs of nodes, and is a measure for global integration of the network. In weighted networks, the average global path length (L_w) is defined by the mean of shortest paths between all possible node pairs in the network, where the shortest path between two vertices is defined as the path with the largest total edge weight.[44,48] Since in a weighted graph, the clustering coefficient and path length are by definition dependent on the weight of the edges and the size of the network, we also calculated the normalized average clustering coefficient () and normalized average shortest path length (L_w) to reduce influence of these properties. The parameters of the original measured networks were than compared to the mean of 50 random networks. Random networks were derived by randomly reshuffling the original edge weights. The clustering and path length were normalized by comparing them to the parameters computed and averaged over 50 surrogate networks: and .11 The clustering coefficient Cw and path length Lw and normalized clustering coefficient $\hat{C}_w$ and path length $\hat{L}_w$ were averaged over all four epochs per subject. The MST and weighted graph analyses were calculated in Brainwave software version 0.9.76, except for the BC per electrode, that was calculated with Brainwave version 0.9.113 (due to change in algorithm producing incorrect results for BC; further information and free available software: http://home.kpn.nl/stam7883/brainwave.html), in four frequency bands (delta band 0.5-4 Hz, theta band 4-8 Hz, alpha band 8-13 Hz and beta band 13-30 Hz).

Statistics

IBM SPSS Statistics version 20 for Mac was used for statistical analyses. Differences between groups in baseline characteristics were tested with χ^2-tests and t-tests where appropriate. We tested the effect of diagnosis and age on degree, leaf fraction, diameter, BC, eccentricity and hierarchy with Analysis of Variance (ANOVA), separately for each frequency band. Network measures were entered as dependent variables, diagnosis and age (young vs. old) were entered as fixed factors and sex was entered as covariate. To correct for multiple comparisons False Discovery Rate (FDR) correction was used.49,50 The

FDR is a method for multiple testing correction that is less conservative than the Bonferroni-correction and it controls for the rate of true detections out of all detections. The first step is to rank the p-values (pi, i = 1, …, N) of all the comparisons (N). Next, we search for the maximum p-value that complies to

$$p_i < \frac{\alpha i}{Nc(N)}$$

where c(N) can be set to 1 and the significance level a = 0.05. All p-values lower than this maximum are considered to be significant detections.[50]

In the main analysis, we used the node with the highest BC to characterize the BC for the whole tree. Since BC is an important measure for the importance of a node within the network, it is also of interest to compare the location of these 'hub-like' nodes between groups. Therefore, we studied in frequency bands with differences between AD patients and controls in an exploratory post-hoc analysis, the MST BC per electrode, with ANOVA for repeated measures. Age was used as between subjects factor and electrode was used as within subjects factor. MST BC was the dependent variable. Sex was entered as covariate. Analyses were stratified for diagnosis. Finally, the association between network characteristics and cognition in AD patients was assessed with Pearson's correlation coefficient. Because the network and connectivity measures are partly dependent on each other we performed Pearson correlation analyses between all measures. MST measures did not show a high correlation with mean PLI across all channels (all $r < 0.6$).

Results

Subject characteristics are summarized in table 1. AD patients were on average older than controls (all $p < 0.01$). There was no difference in gender distribution or MMSE between young and old AD patients and young and old controls. In AD patients, disease duration and disease severity were comparable between young and old. Results of graph theoretical measures of Clustering Coefficient and Path length are summarized in the supplementary material.

Minimum Spanning Tree

Table 2 shows the values of MST measures in four frequency bands with the accompanying ANOVA results. Two-way ANOVA's with diagnosis and age as independent variables showed, after adjustment for sex, main effects of diagnosis on degree, leaf fraction, diameter and eccentricity (all $p \leq 0.001$) in the alpha band. AD patients had a lower maximum degree and leaf fraction and a higher diameter and eccentricity than controls, implying a shift from star-like to line-like topology. Figure 2 shows the average alpha band MST in controls and AD patients. We found no main effect of age on any of the MST measures in the alpha band, or an interaction between diagnosis and age. In the beta, theta and delta band, we found no significant effects of diagnosis or age on MST measures.

Since BC reflects the importance of a single node, we performed post-hoc exploratory ANOVA's for repeated measures on the differences in alpha band BC per electrode, separate for AD patients and controls, to study local differences in hub-nodes according to age. Raw BC values per electrode for the different groups are shown in table 4. In controls, we found neither main effects for age or electrode, nor an interaction between age and electrode. By contrast, in AD patients we found a significant interaction between electrode and age ($F(14.42;4558.13) = 2.35$, $p < 0.01$; main effects of age and electrode not significant), implying a different distribution of hubs in younger compared to older patients. With post-hoc t-tests we examined which electrodes are significantly different between young and old AD patients; these were T3, T5 and O1. Young AD patients had a higher BC in T3 and T5 than older patients and a lower BC in O1 (see figure 3 for MST represented as a tree in young and old AD patients). Figure 4 shows a schematic representation of the difference in BC between young and old AD patients. Both young and old AD patients have a loss of hubs compared to controls, but the regional distribution of hubs is different in young and old AD patients, young patients have stronger hubs than old patients in the left temporal region, while old patients have stronger hubs than young patients in the left occipital region.

Correlation with cognition

Since we only found differences in MST measures in the alpha band, we exclusively studied the correlation with cognitive measures in the alpha band in the group of AD patients. We found several correlations of modest effect size. Higher scores on category fluency were associated with higher diameter ($r = 0.12$, $p < 0.05$) and eccentricity ($r = 0.13$, $p < 0.05$) and lower leaf fraction ($r = -0.13$, $p < 0.05$). Higher scores on VAT recall were associated with lower eccentricity ($r = -0.12$, $p = 0.035$) and diameter ($r = -0.12$, $p = 0.031$) and higher leaf fraction ($r = 0.12$, $p = 0.029$). Worse scores on TMT part B were associated with a lower leaf fraction ($r = -0.14$, $p = 0.045$). Lower scores on digit span backward were associated with lower eccentricity ($r = 0.12$, $p = 0.045$) and diameter ($r = 0.13$, $p = 0.034$). In summary, better scores on VAT recall and TMT part B were associated with a more star-like topology, while better scores on category fluency and digit sp an backward were associated with more line-like topology.

Discussion

With a novel EEG network approach that uses a minimum spanning tree to define network topology, we found loss of hub regions in AD patients compared to controls, reflected by a shift from more integrated star-like to a less integrated line like topology. We found no clear effect of age on global network topology, but we did find a regional difference in centrality measures according to age in AD patients, which was not seen in controls.

Minimum Spanning Tree analysis

When the differences in MST measures between AD patients and controls are placed on the continuum of different tree topologies, from line-like to star-like topology (figure 1), a lower maximum degree in AD patients indicates a shift from a star-like topology to a more line-like topology. A lower leaf fraction in AD patients represents a shift in the same direction. The maximum diameter of a tree decreases with increasing leaf number. In our study, we found that AD patients have a higher diameter compared to controls. This also implies a shift

towards a more line-like topology in AD patients. Together, these measures all point towards a shift from a well integrated star-like to a less integrated line-like topology in AD patients compared to controls. The central node in a star-like network could represent a hub region, and when it gets 'attacked' this will lead to a disruption of efficient information transfer. In line with previous studies on hub regions in AD, a shift to a more line-like topology could be interpreted as a network where the dominant role of hub regions is decreased,10,11 In case of a brain network this translates to a less integrated brain network in AD patients. In a neural mass modelling study, it is shown that the intrinsically high activity level in hub regions predisposes them to activity dependent degeneration (ADD),31 accounting for the targeted attack on hub regions in AD.11 Possibly, in a healthy brain these regions of high connectedness get to process the largest amount of information, making them the most active parts of the brain, and therefore also the most vulnerable.

Regional differences between early and late onset AD

In AD patients, we found regional differences according to age at onset in centrality measures, which could mean that the locations of affected hubs are differently distributed, or that hubs were initially differently affected, causing the emergence of hubs in other locations. Previous studies have shown that hub regions in the human brain correlate highly with areas of vulnerability in AD patients10 and that AD patients have a decreased BC in certain regions compared to controls.[51] The influence of age at onset on hubs in AD has not been studied before. In this study, we found that young AD patients had differences in BC in left hemisphere regions compared to old AD patients, with in the temporal region a higher BC than old AD patients and occipital a lower BC. With a loss of hubs, other regions might become important due to their interconnectedness. It seems these regions differ between young and old AD patients and therefore ADD will also be different, possibly ultimately leading to differences in clinical profile between young and old AD patients. This finding is in line with our previous finding of regional differences in oscillatory brain activity in young and old AD patients.[30] Left hemisphere predominance is also implicated in connectivity and network MEG studies focusing on differences between AD patients and controls.[11,52] The loss of hub regions implicated by a more line-like topology occurs both in young and old AD patients, explaining why we did not find any

global network differences according to age at onset. However, the brain regions where the disruptions take place differ between young and old patients, possibly reflecting a different spatial distribution of hubs between early and late AD, contrary to our prior hypothesis that more hub regions would be affected in early AD. An alternative hypothesis would be that hubs in different locations are affected according to age. This hypothesis is supported by present study and it also coincides with a study on metabolic function in early-onset AD patients from our group, showing a different distribution of loss of glucose metabolism, despite a comparable global decrease.[29] The fact that this study mainly found differences in the parietal cortex, while in the present study, we found differences in centrality measures in the left hemisphere could be due to the different methods. First of all, FDG-PET is an indirect measure of brain activity, by measuring the amount of glucose metabolism in a certain brain region. Secondly, in our study we explore the local brain regions as being part of a network, meaning that not only the local activity is taken into account but also the interactions between all brain regions.

MST in previous studies

The first study that used MST to describe the network characteristics in AD patients was done with functional MRI (fMRI).[53] This study derived an MST from regions within the DMN only, and compared a group of young controls with a group of elderly controls and a group of mild AD patients. In contrast to our study this study found no differences in MST topology between the groups, however they only used degree distribution to define network topology, and only studied the DMN. When they divided the MST in separate clusters, they found that in AD patients the connectivity between the medial temporal lobe and the inferior temporal gyrus was significantly reduced compared to the healthy controls, implying a less efficient network structure in AD patients. Differences between our study and this study might result from the focus of the fMRI study on the DMN, whereas we studied the entire brain, although at a low level of resolution. Another difference between both studies is that the fMRI study was not a resting state study since subjects had to perform a simple task during scanning, which might partially de-activate the DMN. The fMRI study did however find an increased segregation of brain areas, which is in line with our findings.

The MST was used in a previous EEG network study, exploring development of functional brain network topology in young children. It was found that with maturation of the young brain the network shifts away from a centralized star-like network topology towards a more line-like topology.[46] Although this finding coincides with our finding of a shift to line-like topology in AD patients compared to controls, it is very unlikely for these findings to represent a comparable neurophysiological mechanism. Although MST describes patterns of connectivity in both cases, different underlying processes play a role in maturation of developing brains and degeneration of mature brains. Difference between this study and our study is the connectivity measure that is used to construct the MST. The study by Boersma et al. used Synchronization Likelihood (SL) as opposed to the PLI in present study. The SL is a measure that is quite sensitive to volume conduction effects. This may have biased the construction of the MST.

Correlations with cognition

Since cognition depends on the correct integration and segregation of information in the brain, we would have expected to find stronger correlations between network measures and cognition. We found correlations with MST measures and category fluency, VAT recall, TMT part B and digit span backward, all with a correlation coefficient around 0.12, which is a modest effect size. Worse performance on tasks for semantic memory and executive function were associated with a more star-like topology, while worse performance on tasks for short term memory and another task for executive function were associated with a more line-like topology. Although not directly comparable to MST measures, previous studies on connectivity measures using EEG and MEG have variable reports on the correlation with cognition. One study found a negative correlation between connectivity and MMSE in the theta band, which we did not study, however it is not clear in this study whether the correlation was only for the AD patients or for the total group of AD patients and controls.[54] In a study using more specific measures of cognition, namely verbal memory and verbal fluency, correlations between cognition and functional connectivity were found in the alpha and theta band, separate for AD patients and controls.[55] Some studies using network measures have also reported correlations with cognition, for example in an MEG study using eigenvector centrality as network measure a correlation was found in several regions in theta and gamma band connec-

tivity, specifically in AD patients and a study on grey matter networks reported high correlations between path length and cognition.[18,56] However, many EEG or MEG studies did not report whether a correlation between connectivity and cognition was studied, probably resulting in a publication bias.[53,57-59]

Strengths and limitations

Strengths of this study are the use of a large group of AD patients and controls and the use of MST to characterize network topology. The MST offers an elegant solution for problems in thresholding and randomization, making it possible to compare in an unbiased way networks of different sizes and between different groups. It provides a method to construct a unique structure containing the strongest connections in a brain network. This might also be seen as a limitation, since some connections are left out to prevent forming cycles in the network, possibly resulting in a loss of clinical relevant information. Another possible limitation of this study could be the use of PLI as connectivity measure, from which the further network measures were computed. The PLI is a rather strict measure of connectivity, since it discards all (close-to) zero phase lags, thereby also possibly throwing away true connections together with pseudo-connections resulting from volume conduction.[41] Advantage of this method is that the connections that are left are more secure to be genuine connections.

Future directions

In this study, we examined network measures in patients with AD and controls and the association between age of disease-onset. Future studies, preferably longitudinally, in patients at different disease stages are needed to specify where in the disease process changes in brain activity occur and how they relate to other disease mechanisms, for example amyloid pathology. Although EEG is readily available and easy to obtain, it has a relatively low spatial resolution. A good way of measuring brain activity with a higher spatial resolution is magnetoencephalography (MEG).

Conclusion

We investigated the hypothesis that hubs are specifically affected in AD, and explored whether this phenomenon was different in early versus late onset disease. We found evidence of a different network topology, consistent with loss of hubs, in AD irrespective of age. However, the spatial distribution of hub loss was different between early versus late onset AD.

References

1. Rubinov M, Sporns O. Complex network measures of brain connectivity: Uses and interpretations. Neuroimage 2009;

2. Uhlhaas PJ, Singer W. Neural synchrony in brain disorders: relevance for cognitive dysfunctions and pathophysiology. Neuron 2006;52:155-168.

3. Delbeuck X, Van der Linden M, Collette F. Alzheimer's disease as a disconnection syndrome? Neuropsychol Rev 2003;13:79-92.

4. Watts DJ, Strogatz SH. Collective dynamics of 'small-world' networks. Nature 1998;393:440-442.

5. Stam CJ. Functional connectivity patterns of human magnetoencephalographic recordings: a [] small-world' network? Neurosci Lett 2004;355:25-28.

6. Sporns O, Chialvo DR, Kaiser M, Hilgetag CC. Organization, development and function of complex brain networks. Trends Cogn Sci 2004;8:418-425.

7. Gong G, He Y, Concha L, et al.. Mapping anatomical connectivity patterns of human cerebral cortex using in vivo diffusion tensor imaging tractography. Cereb Cortex 2009;19:524-536.

8. Bassett DS, Bullmore E. Small-world brain networks. Neuroscientist 2006;12:512-523.

9. Sporns O, Honey CJ, Kötter R. Identification and classification of hubs in brain networks. PLoS One 2007;2:e1049.

10. Buckner RL, Sepulcre J, Talukdar T, et al.. Cortical hubs revealed by intrinsic functional connectivity: mapping, assessment of stability, and relation to Alzheimer's disease. J Neurosci 2009;29:1860-1873.

11. Stam CJ, de Haan W, Daffertshofer A, et al.. Graph theoretical analysis of magnetoencephalographic functional connectivity in Alzheimer's disease. Brain 2009;132:213-224.

12. Stam CJ, Jones BF, Nolte G, Breakspear M, Scheltens P. Small-world networks and functional connectivity in Alzheimer's disease. Cereb Cortex 2007;17:92-99.

13. Supekar K, Menon V, Rubin D, Musen M, Greicius MD. Network analysis of intrinsic functional brain connectivity in Alzheimer's disease. PLoS Comput Biol 2008;4:e1000100.

14. He Y, Chen Z, Evans A. Structural insights into aberrant topological patterns of large-scale cortical networks in Alzheimer's disease. J Neurosci 2008;28:4756-4766.

15. de Haan W, Pijnenburg YAL, Strijers RLM, et al.. Functional neural network analysis in frontotemporal dementia and Alzheimer's disease using EEG and graph theory. BMC Neurosci 2009;10:101.

16. Yao Z, Zhang Y, Lin L, et al.. Abnormal cortical networks in mild cognitive impairment and Alzheimer's disease. PLoS Comput Biol 2010;6:e1001006.

17. Sanz-Arigita EJ, Schoonheim MM, Damoiseaux JS, et al.. Loss of 'small-world' networks in Alzheimer's disease: graph analysis of FMRI resting-state functional connectivity. PLoS One 2010;5:e13788.

18. Tijms BM, Möller C, Vrenken H, et al.. Single-subject grey matter graphs in Alzheimer's disease. PLoS One 2013;8:e58921.

19. Bokde ALW, Ewers M, Hampel H. Assessing neuronal networks: understanding Alzheimer's disease. Prog Neurobiol 2009;89:125-133.

20. de Haan W, van der Flier WM, Koene T, Smits LL, Scheltens P, Stam CJ. Disrupted modular brain dynamics reflect cognitive dysfunction in Alzheimer's disease. Neuroimage 2011;

21. Chen G, Ward BD, Xie C, et al.. Classification of Alzheimer disease, mild cognitive impairment, and normal cognitive status with large-scale network analysis based on resting-state functional MR imaging. Radiology 2011;259:213-221.

22. Alzheimer's Association. 2010 Alzheimer's disease facts and figures. Alzheimers Dement 2010;6:158-194.

23. Braak H, Braak E. Neuropathological stageing of Alzheimer-related changes. Acta Neuropathol 1991;82:239-259.

24. Seltzer B, Sherwin I. A comparison of clinical features in early- and late-onset primary degenerative dementia. One entity or two? Arch Neurol 1983;40:143-146.

25. Jacobs D, Sano M, Marder K, et al.. Age at onset of Alzheimer's disease: relation to pattern of cognitive dysfunction and rate of decline. Neurology 1994;44:1215-1220.

26. Smits LL, Pijnenburg YAL, Koedam ELGE, et al.. Early onset Alzheimer's disease is associated with a distinct neuropsychological profile. J Alzheimers Dis 2012;30:101-108.

27. Frisoni GB, Pievani M, Testa C, et al.. The topography of grey matter involvement in early and late onset Alzheimer's disease. Brain 2007;130:720-730.

28. Karas G, Scheltens P, Rombouts S, et al.. Precuneus atrophy in early-onset Alzheimer's disease: a morphometric structural MRI study. Neuroradiology 2007;49:967-976.

29. Ossenkoppele R, Zwan MD, Tolboom N, et al.. Amyloid burden and metabolic function in early-onset Alzheimer's disease: parietal lobe involvement. Brain 2012;135:2115-2125.

30. de Waal H, Stam CJ, de Haan W, van Straaten ECW, Scheltens P, van der Flier WM. Young Alzheimer patients show distinct regional changes of oscillatory brain dynamics. Neurobiol Aging 2012;33:1008.e25-1008.e31.

31. de Haan W, Sporns O, Mott K, van Straaten ECW, Scheltens P, Stam CJ. Activity Dependent Degeneration Explains Hub Vulnerability in Alzheimer's Disease PLoS Comput Biol 2012;8:e1002582.

32. de Waal H, Stam CJ, de Haan W, et al.. Alzheimer's disease patients not carrying the apolipoprotein E ε4 allele show more severe slowing of oscillatory brain activity. Neurobiol Aging 2013;

33. Lindeboom J, Matto D. [Digit series and Knox cubes as concentration tests for elderly subjects]. Tijdschr Gerontol Geriatr 1994;25:63-68.

34. Lindeboom J, Schmand B, Tulner L, Walstra G, Jonker C. Visual association test to detect early dementia of the Alzheimer type. J Neurol Neurosurg Psychiatry 2002;73:126-133.

35. REITAN RM. The relation of the trail making test to organic brain damage. J Consult Psychol 1955;19:393-394.

36. Luteijn F, Van der Ploeg FAE. Groninger intelligentie test Handleiding (Groninger Intelligence Test. Manual). Lisse: Swets, Zeitlinger BV 1983;

37. McKhann G, Drachman D, Folstein M, Katzman R, Price D, Stadlan EM. Clinical diagnosis of Alzheimer's disease: report of the NINCDS-ADRDA Work Group under the auspices of Department of Health and Human Services Task Force on Alzheimer's Disease. Neurology 1984;34:939-944.

38. McKhann GM, Knopman DS, Chertkow H, et al.. The diagnosis of dementia due to Alzheimer's disease: recommendations from the National Institute on Aging-Alzheimer's Association workgroups on diagnostic guidelines for Alzheimer's disease. Alzheimers Dement 2011;7:263-269.

39. Petersen RC, Doody R, Kurz A, et al.. Current concepts in mild cognitive impairment. Arch Neurol 2001;58:1985-1992.

40. Nuwer MR. Quantitative EEG: II. Frequency analysis and topographic mapping in clinical settings. J Clin Neurophysiol 1988;5:45-85.

41. Stam CJ, Nolte G, Daffertshofer A. Phase lag index: assessment of functional connectivity from multi channel EEG and MEG with diminished bias from common sources. Hum Brain Mapp 2007;28:1178-1193.

42. Langer N, Pedroni A, Jäncke L. The problem of thresholding in small-world network analysis. PLoS One 2013;8:e53199.

43. van Wijk BCM, Stam CJ, Daffertshofer A. Comparing brain networks of different size and connectivity density using graph theory. PLoS One 2010;5:e13701.

44. van Steen M. Graph Theory and Complex Networks; An Introduction 2010;

45. Kruskal JB, Jr.. On the Shortest Spanning Subtree of a Graph and the Traveling Salesman Problem Proceedings of the American Mathematical Society 1956;7:48-50.

46. Boersma M, Smit DJA, Boomsma DI, De Geus EJC, Delemarre-van de Waal HA, Stam CJ. Growing trees in child brains: graph theoretical analysis of electroencephalography-derived minimum spanning tree in 5- and 7-year-old children reflects brain maturation. Brain Connect 2013;3:50-60.

47. Tijms BM, Wink AM, de Haan W, et al.. Alzheimer's disease: connecting findings from graph theoretical studies of brain networks. Neurobiol Aging 2013;

48. Dijkstra EW. A note on two problems in connexion with graphs Numerische mathematik 1959;1:269-271.

49. Benjamini Y, Hochberg Y. Controlling the false discovery rate: a practical and powerful approach to multiple testing Journal of the Royal Statistical Society. Series B (Methodological) 1995;289-300.

50. Nolte G, Bai O, Wheaton L, Mari Z, Vorbach S, Hallett M. Identifying true brain interaction from EEG data using the imaginary part of coherency. Clin Neurophysiol 2004;115:2292-2307.

51. Seo EH, Lee DY, Lee J-M, et al.. Whole-brain functional networks in cognitively normal, mild cognitive impairment, and Alzheimer's disease. PLoS One 2013;8:e53922.

52. Stam CJ, Jones BF, Manshanden I, et al.. Magnetoencephalographic evaluation of resting-state functional connectivity in Alzheimer's disease. Neuroimage 2006;32:1335-1344.

53. Ciftçi K. Minimum Spanning Tree Reflects the Alterations of the Default Mode Network During Alzheimer's Disease. Ann Biomed Eng 2011;39:1493-1504.

54. Canuet L, Tellado I, Couceiro V, et al.. Resting-State Network Disruption and APOE Genotype in Alzheimer's Disease: A lagged Functional Connectivity Study. PLoS One 2012;7:e46289.

55. Dubovik S, Bouzerda-Wahlen A, Nahum L, Gold G, Schnider A, Guggisberg AG. Adaptive reorganization of cortical networks in Alzheimer's disease. Clin Neurophysiol 2012;124:35 - 43.

56. de Haan W, van der Flier WM, Wang H, Van Mieghem PFA, Scheltens P, Stam CJ. Disruption of functional brain networks in Alzheimer's disease: what can we learn from graph spectral analysis of resting-state magnetoencephalography? Brain Connect 2012;2:45-55.

57. Sankari Z, Adeli H, Adeli A. Intrahemispheric, interhemispheric, and distal EEG coherence in Alzheimer's disease. Clin Neurophysiol 2011;122:897-906.

58. Chan H-L, Chu J-H, Fung H-C, et al.. Brain connectivity of patients with Alzheimer's disease by coherence and cross mutual information of

59. Knyazeva MG, Carmeli C, Khadivi A, Ghika J, Meuli R, Frackowiak RS. Evolution of source EEG synchronization in early Alzheimer's disease. Neurobiol Aging 2012;/n

Table 1. Subject characteristics

	Control			AD		
	All	Young	Old	All	Young	Old
n	245	172	73	319	113	206
Age, years	60 (10)$_a$	55 (7)$_b$	72 (4)$_c$	70 (9)	59 (5)	75 (5)
Sex, female	11 (45)	77 (45%)	34 (47%)	155 (48)	62 (55%)	93 (45%)
Disease duration, years	n.a.	n.a.	n.a.	3.6 (2)	3.8 (2)	3.5 (2)
MMSE	28 (2)$_a$	28 (2)$_b$	29 (1)$_c$	21 (5)	20 (5)	21 (5)

Data are mean (SD) or n (%). $_a$Controls vs. AD patients: $p < 0.01$. $_b$Young control vs. young AD: $p < 0.01$. $_c$Old control vs. old AD: $p < 0.01$

Table 2 (p. 118 / 119). Results ANOVA of MST parameters Raw values of MST measures

Presented data are mean (standard deviation) and accompanying results of ANOVA. Main effect of diagnosis, main effect of age, and interaction between age and diagnosis with F- and p-value. Results that remained significant after correction for multiple comparisons with FDR are printed in bold.

Table 3 (p. 117). Local BC values per electrode.

Presented data are mean (standard deviation). BC values that are significantly different between young and old groups, as analysed with MANOVA, are printed in bold.

Table 3

	Controls		AD	
	Late (n = 73)	Early (n = 172)	Late (n = 206)	Early (n = 113)
Fp2	0.13 (0.13)	0.11 (0.10)	0.13 (0.11)	0.13 (0.11)
Fp1	0.13 (0.14)	0.12 (0.11)	0.12 (0.11)	0.14 (0.11)
F8	0.10 (0.09)	0.11 (0.10)	0.11 (0.10)	0.09 (0.10)
F7	0.10 (0.10)	0.11 (0.10)	0.12 (0.11)	0.12 (0.10)
F4	0.10 (0.10)	0.10 (0.10)	0.12 (0.10)	0.14 (0.11)
F3	0.11 (0.10)	0.10 (0.09)	0.12 (0.11)	0.14 (0.13)
T4	0.10 (0.10)	0.11 (0.10)	0.12 (0.11)	0.10 (0.11)
T3	0.10 (0.11)	0.10 (0.11)	**0.10 (0.10)**	**0.14 (0.12)**
C4	0.16 (0.16)	0.13 (0.12)	0.15 (0.13)	0.13 (0.12)
C3	0.14 (0.12)	0.13 (0.11)	0.14 (0.14)	0.14 (0.12)
T6	0.17 (0.13)	0.16 (0.14)	0.17 (0.14)	0.15 (0.11)
T5	0.14 (0.14)	0.15 (0.15)	**0.16 (0.12)**	**0.21 (0.16)**
P4	0.20 (0.15)	0.18 (0.16)	0.17 (0.14)	0.20 (0.16)
P3	0.16 (0.16)	0.18 (0.15)	0.18 (0.14)	0.18 (0.14)
O2	0.24 (0.16)	0.23 (0.17)	0.22 (0.16)	0.21 (0.16)
O1	0.19 (0.15)	0.22 (0.18)	**0.22 (0.15)**	**0.18 (0.14)**
Fz	0.09 (0.10)	0.11 (0.11)	0.13 (0.10)	0.13 (0.11)
Cz	0.15 (0.12)	0.17 (0.13)	0.15 (0.14)	0.13 (0.11)
Pz	0.22 (0.17)	0.19 (0.16)	0.19 (0.15)	0.18 (0.14)

Table 2

Frequency band	MST measure	Control	AD	Diagnosis		AD vs. Control	Age		Age* Diagnosis	
		Mean (SD)	Mean (SD)	F	P		F	P	F	P
Alpha	Degree	0.330(0.073)	0.302(0.052)	**24.46**	**0.000**	↓	0.03	0.864	1.87	0.172
	Leaf fraction	0.549(0.061)	0.528(0.052)	**15.95**	**0.000**	↓	0.00	0.972	1.19	0.275
	Diameter	0.410(0.047)	0.425(0.045)	**12.60**	**0.000**	↑	0.16	0.689	0.40	0.529
	BC	0.615(0.054)	0.609(0.047)	2.74	0.098		0.31	0.576	0.05	0.827
	Eccentricity	0.312(0.032)	0.322(0.030)	**12.66**	**0.000**	↑	0.18	0.673	0.43	0.513
	Hierarchy	0.455(0.051)	0.442(0.048)	7.83	0.005		0.06	0.804	0.44	0.508
beta	Degree	0.280(0.040)	0.273(0.038)	2.37	0.124		1.25	0.265	0.00	0.977
	Leaf fraction	0.504(0.042)	0.493(0.03)	6.22	0.013		1.56	0.213	1.93	0.165
	Diameter	0.439(0.037)	0.449(0.038)	4.92	0.027		1.45	0.230	0.89	0.346
	BC	0.600(0.046)	0.595(0.044)	1.46	0.228		0.83	0.364	1.67	0.197
	Eccentricity	0.331(0.024)	0.337(0.026)	5.50	0.019		1.47	0.225	1.55	0.214
	Hierarchy	0.427(0.041)	0.422(0.043)	1.31	0.254		0.08	0.772	4.54	0.034

Frequency band	MST measure	Control	AD	Diagnosis		AD vs. Control	Age		Age* Diagnosis	
		Mean (SD)	Mean (SD)	F	P		F	P	F	P
theta	Degree	0.280(0.045)	0.286(0.044)	0.53	0.469		4.64	0.032	0.51	0.477
	Leaf fraction	0.508(0.044)	0.509(0.042)	0.08	0.779		4.23	0.040	0.30	0.587
	Diameter	0.442(0.038)	0.436(0.038)	1.23	0.269		1.38	0.240	0.45	0.504
	BC	0.597(0.048)	0.601(0.046)	0.42	0.517		1.00	0.318	0.80	0.373
	Eccentricity	0.333(0.026)	0.329(0.025)	1.41	0.236		1.27	0.260	0.62	0.432
	Hierarchy	0.433(0.042)	0.431(0.042)	0.23	0.635		0.38	0.539	0.07	0.797
delta	Degree	0.273(0.040)	0.274(0.036)	0.00	0.990		0.13	0.721	4.29	0.039
	Leaf fraction	0.501(0.040)	0.497(0.038)	1.51	0.219		0.00	0.956	2.11	0.147
	Diameter	0.442(0.037)	0.444(0.036)	0.35	0.555		0.06	0.802	2.98	0.085
	BC	0.590(0.043)	0.591(0.042)	0.01	0.909		0.67	0.412	0.45	0.501
	Eccentricity	0.333(0.025)	0.334(0.024)	0.42	0.517		0.05	0.828	3.10	0.079
	Hierarchy	0.432(0.040)	0.431(0.041)	0.57	0.453		0.38	0.540	0.40	0.526

Figure 1

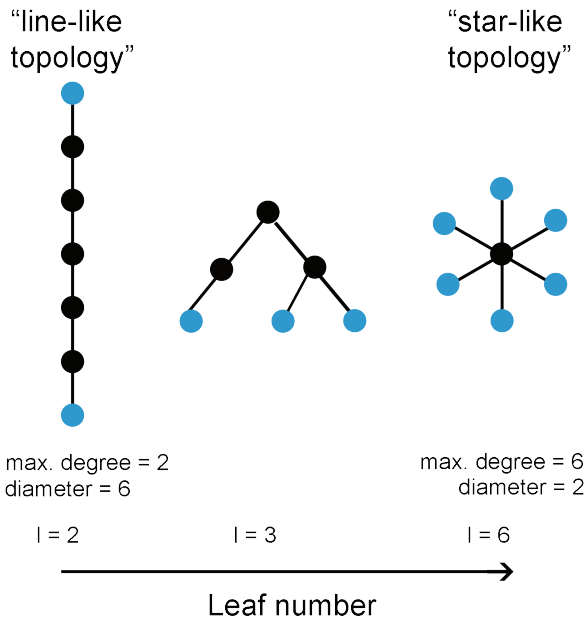

Figure 2

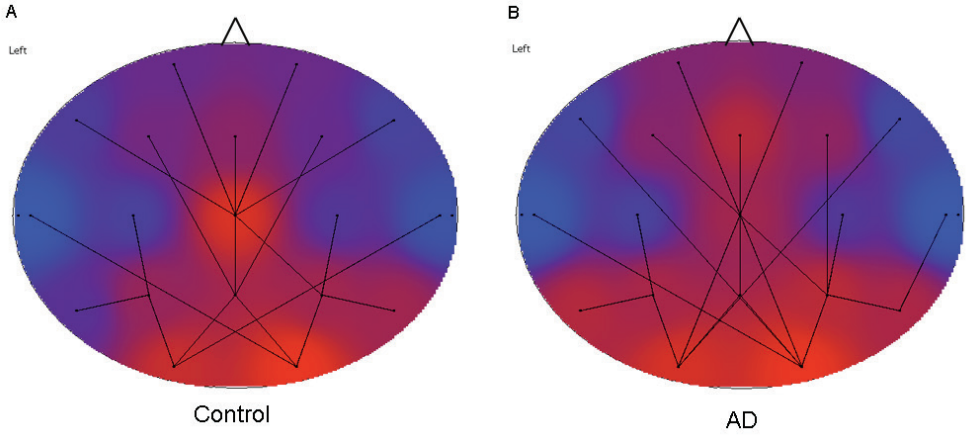

Figure 3

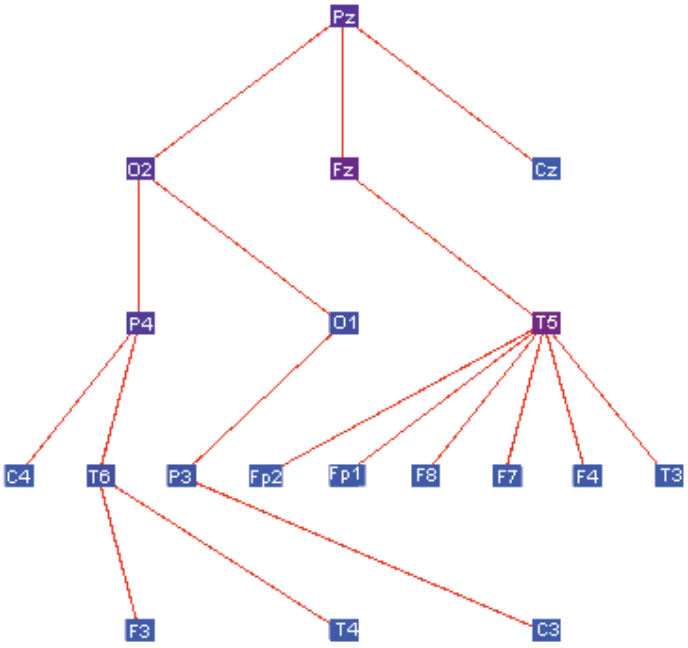

Figure 4

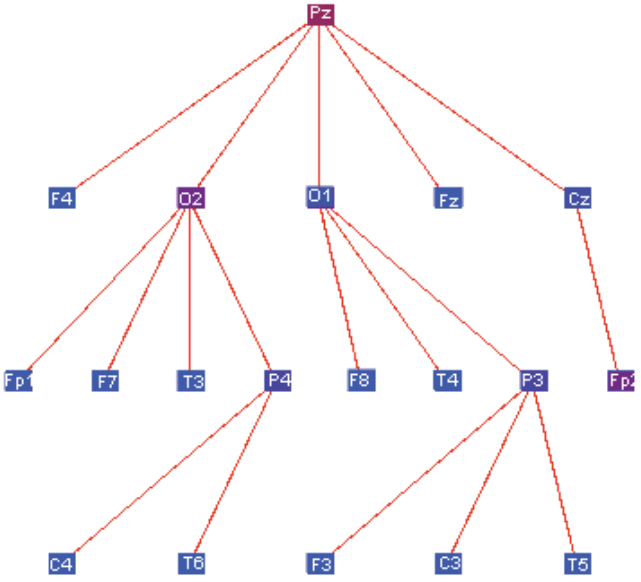

Figure 1 (p. 120). Three minimum spanning trees of the same size (n = 7). The trees on the left and right represent the extreme possible topologies of a minimum spanning tree, in the middle an intermediate tree. Left, a tree with path -like topology, with a minimum possible leaf number of 2 and a maximum degree of 2. The star-like tree on the right has a maximum possible leaf number of 6 (n-1) and a maximum degree of 6. By implementing the formula dmax= m – L + 2 we see that for the path -like tree the diameter dmax = 6 – 2 + 2 = 6 and for the star-like tree dmax = 2 – 2 + 2 = 2.

Figure 2 (p. 120). Alpha band MST of A) control (n = 245) and B) AD patients (n = 319). Underlying colour coding is mean PLI per electrode. Blue means low connectivity, red means high connectivity.

Figure 3 (p. 121). Alpha band MST in A) young AD patients and B) old AD patients represented as a tree.

Figure 4 (p. 121). Difference in Betweenness Centrality (BC) between young AD patients and old AD patients. Areas in red represent higher BC in young AD compared to old AD, areas in blue represent lower BC in young AD compared to old AD.

Supplementary material

Results

First we studied differences in network topology between AD patients and controls by means of the weighted clustering coefficient (C_w) and path length (L_w) and normalized Clustering coefficient (gamma) and normalized path length (lambda)(see table 2). For C_w we found a main effect of diagnosis in the alpha band $p < 0.001$), but no main effect of age nor an interaction between age and diagnosis. AD patients had a lower Cw than controls. In the theta band we found a main effect of age ($p < 0.001$), but no main effect of diagnosis or an interaction between age and diagnosis. Young subjects had a lower Cw than old subjects. In the beta and delta band we found no significant effects. For L_w we found a main effect of diagnosis in the alpha band ($p = 0.001$), but no main effect of age, nor an interaction between age and diagnosis. AD patients had a higher Lw than controls. In the theta band we found a main effect of diagnosis ($p < 0.001$) and a main effect of age ($p < 0.001$), but no interaction between age and diagnosis. AD patients had a lower Lw than controls and young subjects had a higher Lw than old subjects. In the beta and delta band we found no significant effects. To be able to compare network measures between different groups and conditions, we also calculated the normalized network measures gamma and lambda. After correction for multiple comparisons with FDR none of the effects for the normalized graphs remained significant. Because the network and connectivity measures are partly dependent on each other we assessed the Pearson correlation between all measures. We found that the PLI, Cw and Lw form a cluster with correlations higher than 0.9 amongst each other. In other words, any differences in Cw or Lw could be explained by differences in PLI. Note that PLI did not correlate with MST measures.